https://doi.org/10.48048/tis.2025.9467

Combination of Blue Diode Laser and Ag NPs Nanophotosensitizer with Grape Seed Bioreductor to Overcome Biofilm Resistance

Ahmad Khalil Yaqubi[1], Suryani Dyah Astuti[2,*], Nida Ardianti Rakhman[2], Crysant Aquilera[2], Andi Hamim Zaidan[2] and Nasrul Anuar Abd Razak[3]

[1]Doctorate Degree, Department of Physics, Faculty of Science and Technology, Airlangga University, East Java 60115, Indonesia
[2]Department of Physics, Faculty of Science and Technology, Universitas Airlangga, East Java 60115, Indonesia
[3]Department of Biomedical Engineering, University of Malaya, Kuala Lumpur 50603, Malaysia

([*]Corresponding author's e-mail: suryanidyah@fst.unair.ac.id)

Received: 7 December 2024, Revised: 13 January 2025, Accepted: 20 January 2025, Published: 25 March 2025

Abstract

Introduction: Indonesia faces significant health issues due to infection caused by microorganisms. Microbial resistance is increasing, leading to the use of Photodynamic Inactivation, a therapeutic method generating reactive oxygen species. The study evaluates the effectiveness of blue laser and silver nanoparticles synthesized from grape seed as photosensitizers in reducing bacterial biofilms, common pathogens for infections; Materials and methods: The study involved 4 groups of samples: T0, A1 and A2, A3 and A4, and A2 and A4, each exposed to silver nanoparticles and treated with grape seed as a photosensitizer to investigate the effects of laser irradiation on biofilms. The samples were irradiated for 90, 120, 150 or 180 s. Following irradiation, the samples were cultured on TSA media and incubated for 24 h at 37 °C. The number of bacterial colonies was determined using total plate count (TPC). The data obtained were analyzed using a 2-way ANOVA factorial statistical test, followed by Tukey's Post Hoc Test, with $p < 0.05$; Results and discussion: Adding 2 mM, AgNPs-GSE produced the highest percentage of bacterial biofilm inactivation. Specifically, *Escherichia coli* biofilms showed a 72.59 % reduction, while *Staphylococcus aureus* biofilms exhibited an 86.74 % reduction after 180 s of irradiation at a dose of 3.43 J/cm^2; and Conclusions: The study demonstrates that irradiation with a blue diode laser at a dose of 3.43 J/cm^2 for 180 s, combined with the AgNPs-GS photosensitizer, provides bacterial biofilms' most optimal and efficient inactivation.

Keywords: Nanophotosensitizer, AgNPS, Blue laser, Biofilm, Grape seed

Introduction

One of the biggest health problems in Indonesia is infectious diseases. Bacteria such as E *Escherichia coli* (*E. coli*) and *Staphylococcus aureus* (*S. aureus*) are common causes of infections in humans [1]. According to the World Health Organization (WHO) and the United Nations Children's Fund (UNICEF), there are approximately 2 billion cases of diarrhea worldwide each year, and 1.9 million children under 5 years old die from diarrhea annually [2]. *E. coli* is a typical bacterium in the intestines, but when present in excessive amounts, it can cause diarrhoea. If this bacterium spreads to other organ systems, it can lead to infections [3]. *E. coli* infections often present with diarrhoea, blood in the stool, stomach cramps, fever, and, in some cases, kidney problems [4].

S. aureus is a gram-positive bacterium that plays a significant role in causing diseases on the human skin [5]. It is usually present in the mouth and respiratory tract but can become pathogenic under certain conditions. *S. aureus* has facultative anaerobic properties, allowing it to reproduce and spread throughout the body [6]. It also produces several

extracellular substances that contribute to various diseases and can form biofilms, which protect the bacteria from external threats [7]. Infections caused by *S. aureus* can result from direct contamination, such as in post-surgical wound infections or infections following trauma [8].

Antibiotics are substances produced by organisms that can inhibit the growth of other organisms [9]. According to WHO data, global antibiotic use increased by 91 and 165 % in developing countries from 2000 to 2015 [10]. *E. coli* and *S. aureus* can form biofilms that are highly resistant to commercially available antibiotics, which poses a significant challenge in medical therapy [11]. Research has shown that *E. coli* and *S. aureus* resist almost all antibiotics tested [12]. To address this, many researchers have explored new methods to develop more efficient antimicrobials that can overcome microbial resistance at lower costs [13].

Nanotechnology has emerged as a promising solution with the rapid advancement of science and technology [14]. This technology utilizes antibacterial properties, including those of metal nanoparticles and low-dose antibiotics [15]. Nanotechnology involves working with atoms and molecules sized smaller than 1,000 nm. Nanoparticles, which range from 1 to 100 nm, have a large surface area, enhancing their ability to interact with other substances [16]. Metal nanoparticles exhibit antimicrobial activity because they can bind to protein molecules in microbial cells, disrupting microbial metabolic processes and leading to cell death [17]. These nanoparticles can be derived from various materials, including platinum, gold, silver and palladium [18]. Among these, silver nanoparticles are the most widely used due to their unique properties, ease of use, and ability to bind to various biomolecules, making them effective in killing bacteria, fungi and biofilm [19,20].

Silver nanoparticles, also known as AgNPs, possess unique properties, including high electrical and thermal conductivity, chemical stability and broad-spectrum bactericidal and fungicidal activity [21]. These nanoparticles can be used in liquid form, such as colloids and solid form [22]. They are also applied in textiles, membrane filtration and water purification systems [23]. Factors influencing the particle size during synthesis include solution temperature, salt concentration, reducing agents and reaction time. Silver nanoparticles can be synthesized using physical, chemical or biological methods [24]. Some chemical methods include co-precipitation, sol-gel, electrochemistry, hydrothermal synthesis and spray drying. However, these methods often present challenges, such as hazardous chemicals, expensive reagents and high energy consumption [25]. The green synthesis method has been chosen to address these issues, utilizing plant extracts as reducing agents in line with environmentally friendly principles [26].

Green synthesis, also known as environmentally friendly synthesis, is a sustainable method that utilizes natural materials as precursors, helping to reduce pollutants and minimizing potential dangers to researchers and the environment [27]. This method is advantageous because natural materials are widely available, inexpensive and non-toxic [28]. In green synthesis, natural materials function as capping agents or stabilizers for the crystal structure [29]. This method has 3 critical factors: The solvent, the reducing agent and the non-toxic material. One significant advantage of this approach is that the shape and size of the nanoparticles can be tailored to specific requirements [30].

Additionally, amino acids, proteins and secondary metabolites are produced during the synthesis process, and the stages are shortened to prevent aggregate formation [31]. The bioreactors used in green synthesis are derived from natural materials that contain antioxidant compounds or polyols, which can reduce silver ions [32]. Plants play a crucial role in the synthesis process, utilizing organic compounds, especially secondary metabolites like terpenoids, flavonoids and tannins, which possess antioxidant properties [33].

One plant that can be used for this purpose is grape seed. Grape seeds contain saponins, alkaloids and flavonoids [34]. The extract forms an orange precipitate, indicating the presence of flavonoid compounds, though in small amounts [35]. Flavonoids are a group of phenolic compounds with antioxidant properties, as they strongly tend to reduce metals [36]. The ability of phenolic compounds to chelate and reduce metals is attributed to the high nucleophilic character of the aromatic ring. The reduction of silver nanoparticles occurs through the oxidation of plant extract phenolic compounds [37]. Ag^+ ions interact to form silver nanoparticles, which are stabilized by phenolic

derivatives and other ligands found in plants [38]. Silver nanoparticles exhibit an intense absorption spectrum at wavelengths between 400 and 500 nm [39].

Silver nanoparticles can be nano photosensitizers in antimicrobial photodynamic therapy (PDT). Photosensitizers are chemical compounds or agents that are sensitive to light and are used in various applications, including photodynamic therapy, medical diagnosis and cancer treatment [40]. Generally, photosensitizers absorb electromagnetic radiation, including infrared, visible light and ultraviolet radiation. Organic photosensitizers tend to have micro-sized particles, which make it difficult for them to penetrate the biofilm due to the extracellular polymeric substance (EPS) matrix. Therefore, nano-sized particles are more effective in targeting biofilms [41]. aPDT is a treatment method that combines light with a photosensitizing agent to produce a photochemical reaction that damages microorganisms such as bacteria, viruses, and fungi *in vitro* [42] and *in vivo* [43]. The success of aPDT depends on 3 components: The photosensitizer (PS), light with a spectrum that matches the absorption spectrum of the photosensitizer and oxygen. When the photosensitizer absorbs light energy, it triggers intersystem crossing and photochemical reactions with biological substrates or oxygen, producing reactive oxygen species (ROS) through energy transfer and charge transfer. These ROS then cause damage to lipids and cell membrane proteins, leading to cell lysis [44,45].

The light emitted by the blue diode laser (405 nm) is absorbed by photosensitizers such as silver nanoparticles (AgNPs), producing reactive oxygen species (ROS) that kill bacterial cells oxidatively. However, the blue diode laser needs a photosensitizer to be very effective and has little bactericidal action. Power and exposure duration are 2 characteristics that affect the laser's efficacy. On the other hand, silver nanoparticles work against microorganisms in several ways. Membrane rupture, protein damage and DNA destruction result from their binding to bacterial cell walls, release of silver ions, and generation of reactive oxygen species (ROS). Because of their higher surface area, smaller nanoparticles of AgNPs often exhibit superior action against a wider variety of bacteria, including *E. coli* and *S. aureus*. By interacting directly with bacteria and generating reactive oxygen species (ROS), AgNPs have higher bactericidal activity than the blue diode laser alone, which only has mild antimicrobial effects.

A laser is a light source that emits a coherent beam at a specific wavelength. A diode laser is a device capable of emitting coherent, focused and monochromatic photons. Several previous studies have demonstrated the efficacy of diode laser-based antimicrobial photodynamic therapy (aPDT) in inactivating bacteria and biofilms and accelerating wound healing [46]. The effectiveness of aPDT depends on the alignment of the light source's spectrum with the absorption spectrum of the photosensitizer, as well as the intensity and energy of the exposed photons. This research aims to enhance the effectiveness of blue laser aPDT (405 nm) by incorporating grape seed extract silver nanoparticle photosensitizers (AgNPs-Gs) to reduce bacterial biofilms responsible for infections, including the gram-negative *E. coli* and gram-positive *S. aureus*.

Materials and methods

Synthesis and preparation of silver nanoparticles

The natural material used in this research is grape seed. Sample preparation involved extracting grape seed. Grape seed powder (0.2 g) was weighed accurately, and 10 mL of an ethanol-water solvent (70:30, v/v) was added, followed by placement in a microwave. The power used was 10 % of the total electrical power (900 W), and the irradiation time was maintained for 9 min. After microwave-assisted extraction, the extract was centrifuged at 5,000 rpm for 30 min. The supernatant was diluted with 10 mL of ethanol-water solvent (70:30, v/v) in a 25 mL volumetric flask.

The synthesis of Piper scrotum silver nanoparticles (AgNPs-Gs) was performed using the green synthesis method based on modified procedures from previous studies [47,11]. Prior to synthesis, variations in the concentration of the $AgNO_3$ solution were prepared by dissolving 0.0425 g of $AgNO_3$ crystal powder for a 1 mM concentration, 0.064 g for a 1.5 mM concentration, and 0.085 g for a 2 mM concentration, each in 250 mL of distilled water. Then, 2 mL of grape seed extract was mixed with 18 mL of $AgNO_3$ solution at varying concentrations (1, 1.5 and 2 mM) in an Erlenmeyer flask. The flask was covered with aluminum

foil and placed in a microwave at 40 % of 900 W electrical power and a frequency of 2,450 MHz, with a synthesis time of 5 min. The synthesis of AgNPs-Gs was complete when the solution colour changed to yellowish-brown and became homogeneous. The AgNPs-Gs were then characterized using a UV-Vis spectrophotometer. The formation of silver nanoparticles was indicated by the colour change of the solution from clear to brownish-yellow [48].

Bacterial culture

E. coli and *S. aureus* bacteria were cultured in Tryptone Soy Broth (TSB) and incubated for 24 h at 37 °C until the colony reached a 1.0 McFarland standard.

Laser source

The light source used was a blue laser diode with a wavelength of 405 nm. Characterization was performed using a Jasco CT-10 monochromator to determine the peak wavelength. The power output was 2.49 MW, measured with an OMM-6810B-220V power meter. The spot beam area had a size of 0.13 cm^2. Diode laser irradiation was carried out with varying exposure times of 90, 120, 150 and 180 s. The irradiation time was determined as follows to calculate the energy density [49].

$$\text{Energy density } (\text{J} \cdot \text{cm}^{-2}) = \text{Intensity } (\text{W} \cdot \text{cm}^{-2}) \times \text{Irradiation Time (s)}$$

Antibacterial activity test

This test was conducted to determine whether the antibacterial compounds in silver nanoparticles synthesized with grape seed extract could increase the mortality of bacterial colonies. The disc diffusion (or cup) method was used to test antibacterial activity. A 50 μL bacterial culture sample was taken, and Tryptic Soy Agar (TSA) was added to a petri dish [50]. A paper disc was treated with 10 μL of grape seed extract. After the paper disc absorbed the solution, it was placed onto the surface of the agar medium in the petri dish. The petri dish was then incubated for 24 h. The presence of an inhibitory zone around the paper disc indicated the antibacterial activity of grape seed extract.

Illumination treatment

The experiment involved 4 groups of samples. The first group, the control group (T0), consisted of samples without laser irradiation. The second group included *E. coli* samples in group A1, which were irradiated with a 405 nm diode laser at varying irradiation times, and group A2, treated with varying concentrations of silver nanoparticles for 10 min. The third group contained *S. aureus* samples, with group A3 irradiated with a 405 nm diode laser at different irradiation times and group A4 treated with varying concentrations of silver nanoparticles for 10 min. The fourth group consisted of bacterial samples from groups A2 and A4, each supplemented with grape seed photosensitizer (PS). The laser treatment groups were irradiated for 90, 120, 150 and 180 s. After treatment, all samples were plated on TSA media and incubated for 24 h at 37 °C. The number of bacterial colonies was then counted using the total plate count (TPC) method.

Statistical analysis

The results obtained will be recorded as statistical data. Statistical analysis was performed using IBM SPSS (Statistical Package for the Social Sciences). A 2-way ANOVA factorial test was conducted to determine the influence of each factor and the interactions between factors. The conditions for performing the 2-way ANOVA factorial test are that the data must be normally distributed, the data variations must be homogeneous, and the data should be on a minimum interval scale. The null hypothesis (H0) is rejected if the *p*-value is less than $\alpha = 0.05$. A Tukey post-hoc test was also carried out to identify differences between each sample factor, with the condition that $p < 0.05$. Based on the data obtained and the statistical analysis performed, the most effective radiation treatment for inactivating *E. coli* and *S. aureus* bacteria will be identified.

Results and discussion

Grape seed extract was used as the reductant, obtained through microwave irradiation and centrifugation. The resulting extract is yellowish, as shown in **Figure 1(a)**, with an absorption spectrum peak at a wavelength of 360 nm. **Figures 1(b)** - **1(c)** shows the Grape seed extract silver nanoparticles.

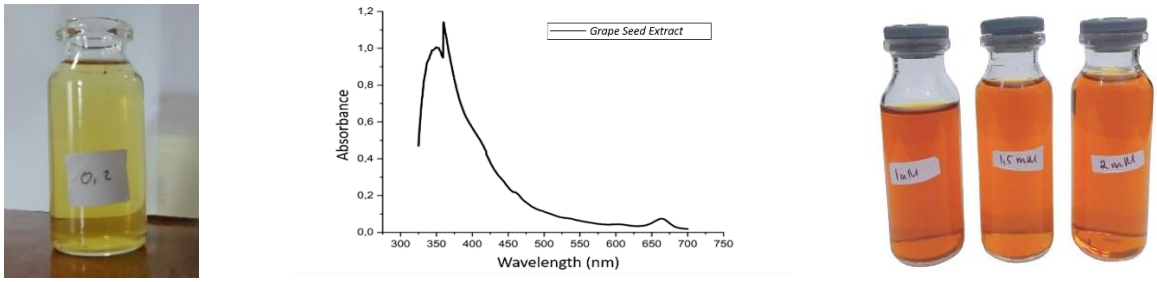

(a) (b) (c)

Figure 1 (a) Grape seed extract; (b) UV-Vis spectrum of grape seed extract; (c) silver nanoparticles synthesized using grape seed extract.

The green synthesis process, involving the mixing of the reductant with varying concentrations of $AgNO_3$ (1, 1.5 and 2 mM), causes a colour change from the original colorless $AgNO_3$ solution and the yellowish Grape seed extract to a brownish hue, as shown in **Figure 1(c)**. This colour change indicates the reduction of Ag^+ to Ag^0, signaling the formation of nanoparticles [51].

Characterization of the Grape seed extract silver nanoparticles (AgNPs) included 4 tests: UV-Vis, PSA, stability and FTIR. UV-Vis characterization was performed to evaluate the ability of Grape seed extract silver nanoparticles to absorb light at different wavelengths, ranging from 325 to 700 nm. The peak absorption spectrum of the Grape seed extract silver nanoparticles occurred at a wavelength of 425 nm, with an absorbance of approximately 1.7, as shown in **Figure 2**. Based on this absorbance value, the percentage of light absorbed by the photosensitizer during blue laser irradiation can be calculated using the Lambert-Beer equation, which yielded an absorption rate of 81.7 %.

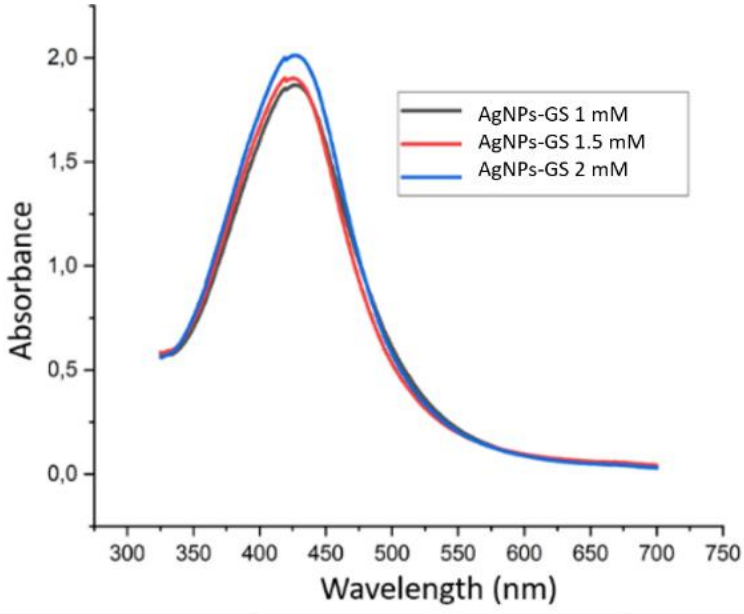

Figure 2 Absorbance spectrum of grape seed extract silver nanoparticles at concentrations of 1, 1.5 and 2 mM.

The Particle Size Analyzer (PSA) was used to measure the size distribution of nanometer-sized particles. The PSA results for Grape seed extract AgNPs at concentrations of 1, 1.5 and 2 mM were 118.36, 100.79 and 128.71 nm, respectively (**Figure 3**).

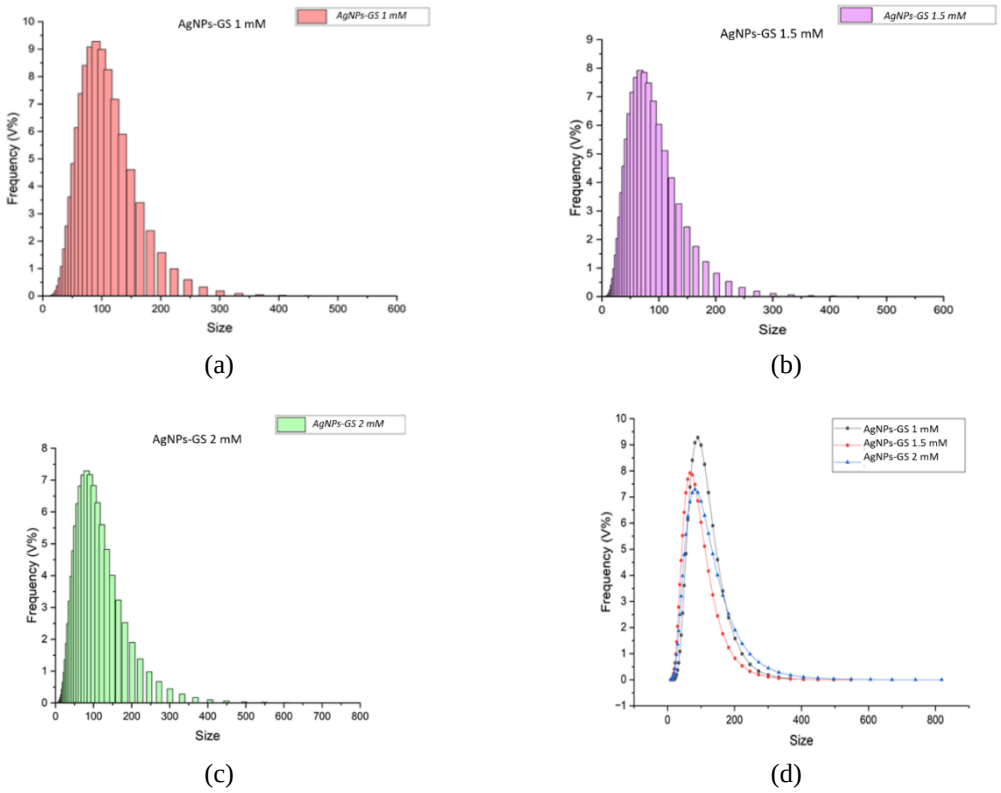

Figure 3 PSA test results for AgNPs (a) 1 mM, (b) 1.5 mM, (c) 2 mM and, (d) comparison of the 3 concentration variations.

These results indicate that the synthesized Grape seed AgNPs fall within the nanoparticle size range. The dispersion index (PDI) values for each concentration were 0.20, 0.29 and 0.35, respectively. The PDI describes the particle size variability in a sample, and a PDI value between 0.01 and 0.7 indicates a homogeneous or uniform particle size distribution. The more homogeneous the particle size, the more stable the nanoparticles are. To test the stability of the nanoparticles, the Grape seed AgNPs were observed from day 1 to day 7, as shown in **Table 1**. The physical observation results indicated a colour change to a darker, brownish hue, with no visible agglomeration throughout the 7 days, suggesting the nanoparticles remained stable.

Table 1 Comparison of physical properties and absorption spectrum of silver nanoparticle synthesis from Grape seed extract from day 1 to day 7.

Day	Sample	Description	Absorbance spectrum
1		Golden brown	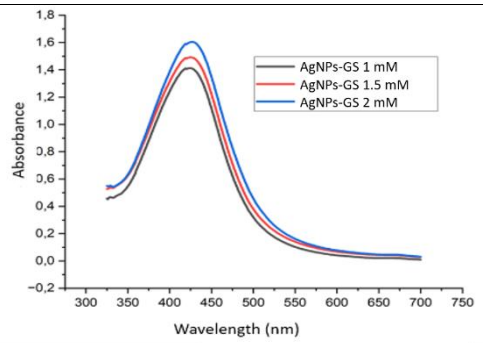
2		Golden brown	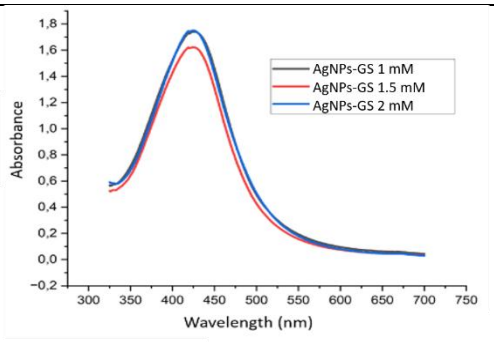
3		Golden brown	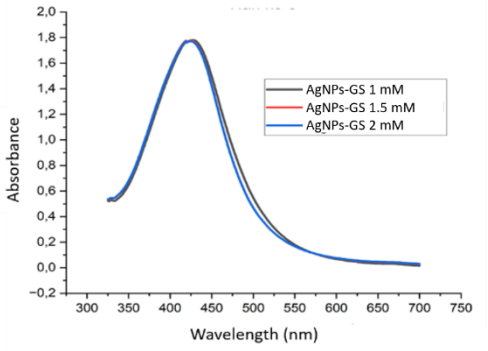
4		Chocolate	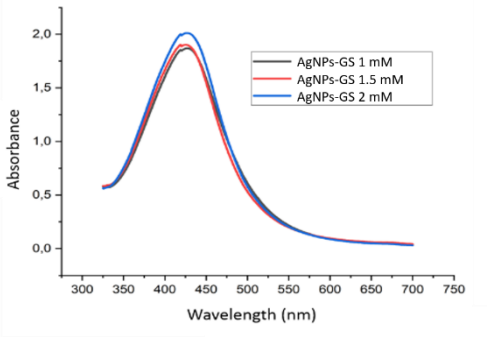

Day	Sample	Description	Absorbance spectrum
5		Chocolate	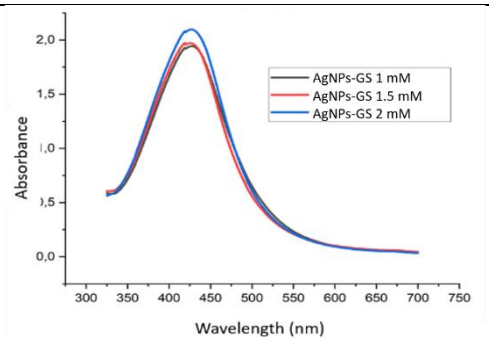
6		Cloudy brown	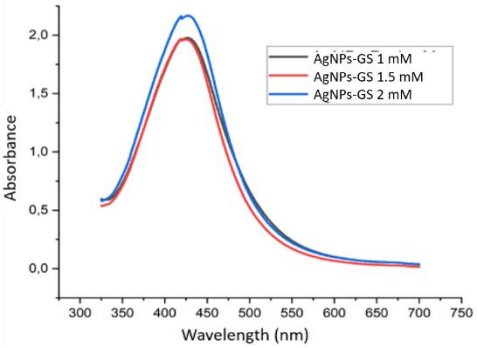
7		Cloudy brown	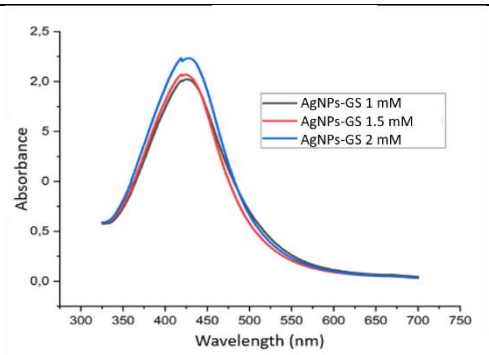

Fourier Transform Infrared Spectroscopy (FTIR) characterization was performed to identify the functional groups in Grape seed AgNPs, which act as bioreductants for the biosynthesis of silver nanoparticles. This analysis also provides information on the formation of AgNPs-Gs. The results of the FTIR characterization are presented in **Figure 4** and **Table 2**.

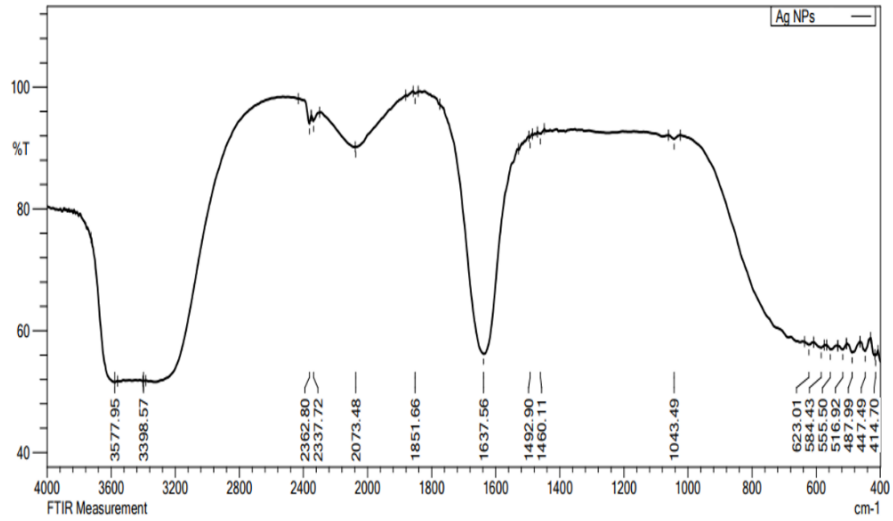

Figure 4 FTIR results of AgNPs-Gs samples with a concentration of 2 mM.

Table 2 Results of laboratory analysis using FTIR.

No.	Wave value (cm^{-1})	Function group
1	3,577.95	Tertiary alcohol, OH stretch Phenols, OH stretch
2	3,398.57	Alkyne C-H stretch
3	2,073.48	Transition metal carbonyls Isothiocyanate (-NCS) Cyanide ion, thiocyanate ion, and related ions
4	1,637.56	Alkenyl C=C stretch Primary amine, NH bend Secondary amine, > N-H bend Amide
5	623.01	Alkyne C-H bend
6	584.43; 555.50; 516.92	Aliphatic iodo compounds, C-I stretch
7	487.99	Polysulfides (S-S stretch)
8	447.49	Aryl disulfides (S-S stretch)

Based on **Figure 4** and **Table 2**, the FTIR spectrum of AgNPs-Gs shows absorption peaks at 3,577.95, 3,398.57, 2,073.48, 1,637.56, 623.01, 584.43, 555.50, 516.92, 487.99 and 447.49 cm^{-1}. These peaks indicate the presence of secondary metabolite compounds such as flavonoids, steroids, alkaloids and tannins in AgNPs-Gs, which act as reductants for silver ions and stabilizing agents. Flavonoids, which contain O-H groups, are identified by the hydroxyl groups in the reducing agents [52]. The FTIR results show an O-H group at 3,577.95 ccm^{-1}, a characteristic feature of flavonoids. Also, alkaloids contain an O=C-N (amide carbonyl) group, observed at 1,637.56 cm^{-1}. Thus, the FTIR characterization indicates that AgNPs-Gs contain secondary metabolites, specifically flavonoids and alkaloids, as reductants for silver metal ions.

The antibacterial activity of AgNPs-Gs was tested using the disk diffusion method, examining the inhibition zone in bacterial colony growth. The inhibition zone forms when AgNPs-Gs spread across the medium and kill or inhibit bacterial growth. The antibacterial test results against *E. coli* and *S. aureus* bacteria, as shown in **Figure 5**, reveal inhibition zones around the paper disc areas treated with AgNPs-Gs at 1,

1.5 and 2 mM. For *E. coli*, the inhibition zones measured 0.56, 0.84 and 0.92 mm, respectively. In the case of *S. aureus*, the inhibition zones were 1.34, 1.44 and 1.59 mm at concentrations of 1, 1.5 and 2 mM, respectively.

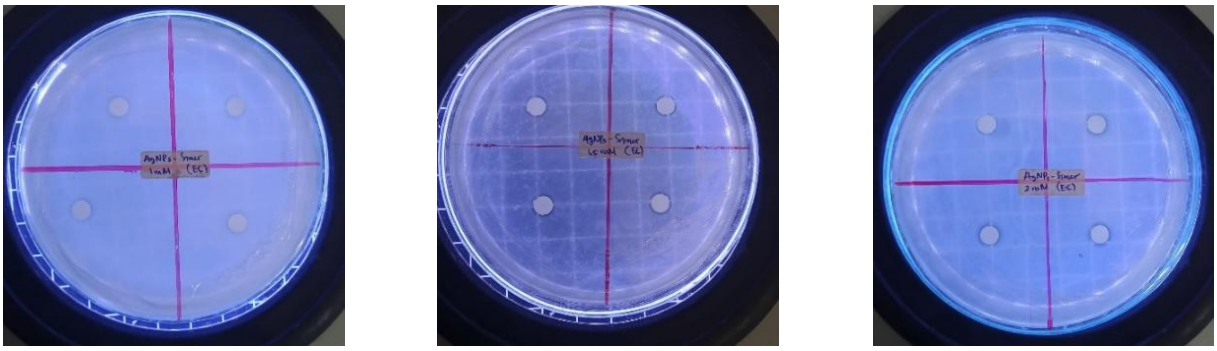

(a) Inhibition zone: 0.56 mm (b) Inhibition zone: 0.84 mm (c)Inhibition zone: 0.92 mm

(A)

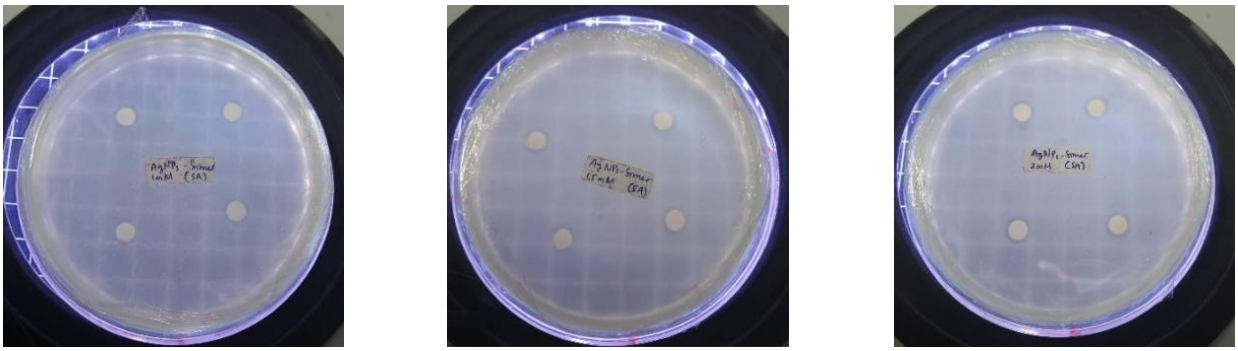

(a) Inhibition zone: 1.34 mm (b) Inhibition zone: 1.44 mm (c) Inhibition zone: 1.59 mm

(B)

Figure 5 (A) Antibacterial test results of AgNPs-Gs (a) 1 mM, (b) 1.5 mM and (c) 2 mM using the disk diffusion method against *E. coli* bacteria (B) Antibacterial test results of AgNPs-Gs (a) 1 mM, (b) 1.5 mM and (c) 2 mM using the disk diffusion method against *S. aureus* bacteria.

Adding AgNPs-Gs to 2 different bacterial samples demonstrated that the synthesized nanoparticles possess antibacterial properties. Bacterial growth was measured by counting the number of colonies that grew when AgNPs-Gs were applied to the plate. **Figures 6(a) - 6(b)** show the percentage reduction in *E. coli* and *S. aureus* bacterial colonies. AgNPs-Gs exhibited an inhibitory effect on bacterial growth, as indicated by the results shown in both figures.

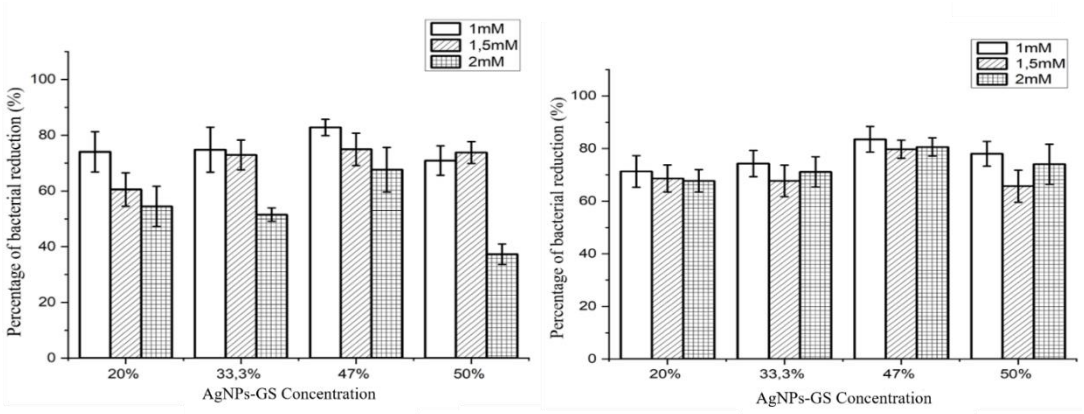

Figure 6 (a) Percentage reduction of *E. coli* bacteria at various concentrations of AgNPs-Gs and (b) percentage reduction of *S. aureus* bacteria at various concentrations of AgNPs-Gs.

Laser irradiation was conducted at 4-time variations, with different intensities and doses. The success of the process was measured by reducing bacterial colonies. Treatment groups included laser-only and laser-added 47 % AgNPs-Gs photosensitizer groups, and the results were compared with the control group.

The study demonstrates that blue laser irradiation on *E. coli* bacteria decreases the number of viable colonies compared to the control group. However, AgNPs-Gs photosensitizer significantly reduces the number of colonies after 180 s of exposure. The results suggest a relationship between energy density and bacterial viability, with AgNPs-Gs photosensitizer enhancing the laser's effect on reducing bacterial colonies.

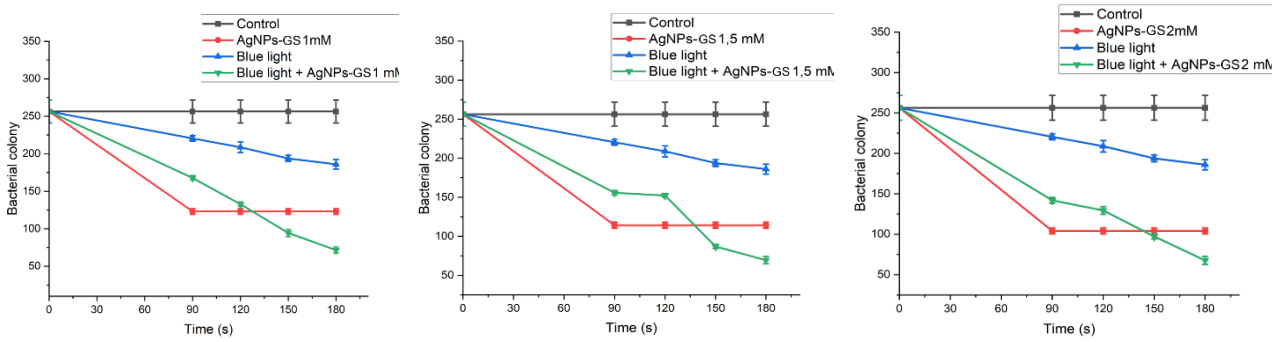

Figure 7 Graph of decreasing viability of *E. coli* bacteria after blue laser irradiation and addition of AgNPs-Gs with concentrations of (a) 1 mM, (b) 1.5 mM and (c) 2 mM.

The data was analyzed using the 2-way ANOVA factorial test in IBM SPSS. The results showed that the data was normally distributed and homogeneous. The treatment groups showed significant differences, with the AgNPs-Gs concentration group showing the most effective reduction. A post hoc test showed no significant difference between the AgNPs-Gs concentration groups, but the exposure time variation and interaction group showed significant differences.

Table 3 Results of statistical analysis on *E. coli* bacteria.

Treatment	Group	N	Bacterial death (%)		ANOVA	
			Average	SD	Signification	Conclusion
AgNPs-Gs concentration	1 mM (a)	20	57.7	15.5	0.765	There is no significance difference
	1.5 mM (a)	20	52.92	16.5		
	2 mM (a)	20	55.78	12.4		
Exposure time	90 s (a)	15	37.06	5.2	0.000	There is a significance difference
	120 s (b)	15	43.99	5.3		
	150 s (c)	15	62.34	3.1		
	180 s (d)	15	71.8	2.6		
Interaction	1 mM 90 s (a)	5	31.96	2.4	0.000	There is a significance difference
	1 mM 120 s (c)	5	46.15	3.3		
	1 mM 150 s (d)	5	61.72	2.0		
	1 mM 180 s (e,f)	5	70.97	3.3		
	2 mM 90 s (a,b)	5	36.82	2.1		
	2 mM 120 s (a,b)	5	38.28	3.4		
	2 mM 150 s (d,e)	5	64.72	3.5		
	2 mM 180 s (f)	5	71.86	2.9		
	3 mM 90 s (b,c)	5	42.42	3.9		
	3 mM 120 s (c)	5	47.53	3.8		
	3 mM 150 s (d)	5	60.58	2.5		
	3 mM 180 s (f)	5	72.59	1.5		

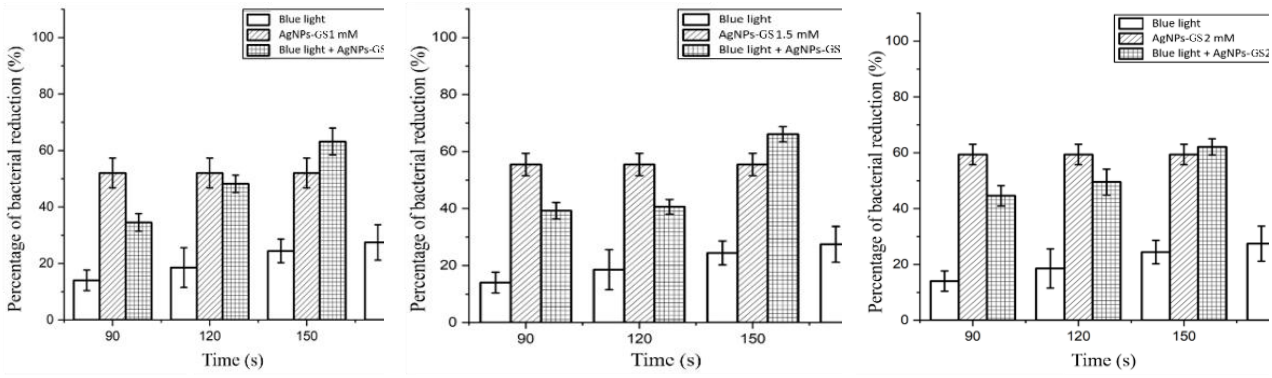

(a) (b) (c)

Figure 8 Comparison of the percentage reduction of *E. coli* bacteria with AgNPs-Gs (a) 1 mM, (b) 1.5 mM and (c) 2 mM.

The study found no significant difference in the concentration of AgNPs-Gs between the 3 treatment groups, but significant differences were observed in the exposure time variation and interaction groups. The most effective treatment group in reducing *E. coli* bacterial biofilm colonies was AgNPs-Gs with a concentration of 2 mM and 180 s of exposure, resulting in a bacterial death percentage of 72.59 %.

The study demonstrates that blue laser irradiation of *S. aureus* bacteria decreases the number of bacterial colonies compared to the control group. However, the blue laser treatment with AgNPs-Gs photosensitizer significantly reduces the number of live colonies. The

study also found that laser irradiation enhances the effectiveness of AgNPs-Gs photosensitizer in reducing bacterial colonies at concentrations of 1, 1.5 and 2 mM.

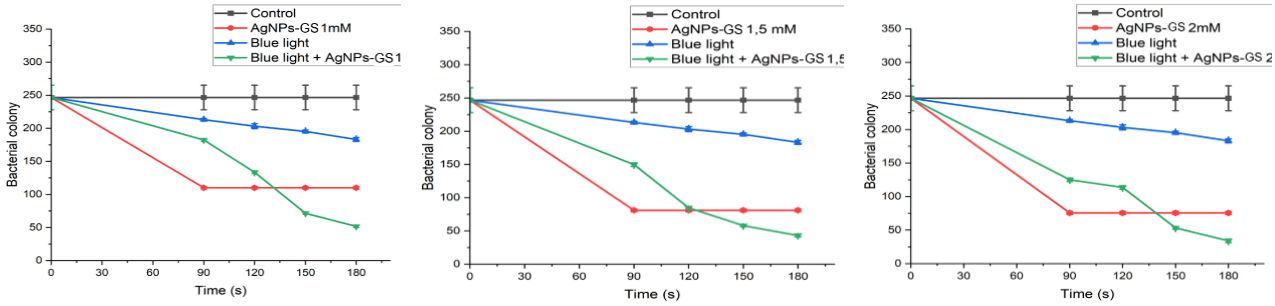

(a) (b) (c)

Figure 9 Graph of decreasing viability of *S. aureus* bacteria after blue laser irradiation and addition of AgNPs-Gs with concentrations of (a) 1 mM, (b) 1.5 mM and (c) 2 mM.

The results of the data normality test for the 3 treatment groups showed a significance value of $p = 0.143 > \alpha = 0.05$, indicating that the data is usually distributed. Meanwhile, the homogeneity test results showed a significance value of $p = 0.762 > \alpha = 0.05$, which means the data is homogeneous. The results of the 2-way ANOVA factorial analysis for the AgNPs-Gs concentration group, the variation in the exposure time group, and the interaction group all showed a significance value of $p = 0.000 < \alpha = 0.05$, indicating significant differences between the treatment groups. As a result, a post-hoc test was performed on the 3 treatment groups. The post-hoc test results showed that the AgNPs-Gs concentration groups were not significantly different from each other. However, the exposure time variation group and the interaction group showed significant differences, as shown in **Table 4**.

Table 4 Results of statistical analysis on *S. aureus* bacteria.

Treatment	Group	N	Bacterial death (%)		ANOVA	
			Average	SD	Signification	Conclusion
AgNPs-Gs concentration	1 mM (a)	20	57.22	20.8	0.106	There is no significance difference
	1.5 mM (a)	20	67.28	16.5		
	2 mM (a)	20	68.21	15.7		
Time	90 s (a)	15	40.56	9.9	0.000	There is a significance difference
	120 s (b)	15	56.87	8.7		
	150 s (c)	15	76.26	3.9		
	180 s (d)	15	83.26	3.4		
Interaction	1 mM 90 s (a)	5	28.86	3.0	0.000	There is a significance difference
	1 mM 120 s (c)	5	47.97	3.7		
	1 mM 150 s (e,f)	5	72.15	1.9		
	1 mM 180 s (g)	5	79.88	1.4		
	1.5 mM 90 s (b)	5	41.65	3.2		
	1.5 mM 120 s (e)	5	66.93	3.8		
	1.5 mM 150 s (f,g)	5	77.38	2.8		

Treatment	Group	N	Bacterial death (%)		ANOVA	
			Average	SD	Signification	Conclusion
	1.5 mM 180 s (g,h)	5	83.15	1.8		
	1.5 mM 90 s (c,d)	5	51.17	3.0		
	1.5 mM 120 s (d)	5	55.69	2.9		
	1.5 mM 150 s (g)	5	79.25	2.9		
	1.5 mM 180 s (h)	5	86.74	2.5		

The 2-way ANOVA factorial analysis results for the AgNPs-Gs concentration group showed a significance value of $p = 0.106 > \alpha = 0.05$, indicating no significant difference. The treatment group with variations in laser irradiation time showed a significance value of $p = 0.000 < \alpha = 0.05$, indicating a significant difference between the treatment groups. The interaction group treatment showed a significance value of $p = 0.000 < \alpha = 0.05$, indicating significant differences between the treatment groups. As a result, a post-hoc test was conducted for the 3 treatment groups. The post-hoc test results showed that the AgNPs-Gs concentration groups were not significantly different from each other. However, the exposure time variation and interaction groups showed significant differences, as shown in **Table 4**. Based on the results of this analysis, the most effective treatment for reducing *S. aureus* bacterial colonies was 1.5 mM with 180 s of exposure (or a dose of 3.34 J/cm^2), resulting in a bacterial death percentage of 86.74 %. **Figure 10** shows the comparison of the percentage reduction of *S. aureus* bacteria with AgNPs-Gs (a) 1 mM, (b) 1.5 mM and (c) 2 mM.

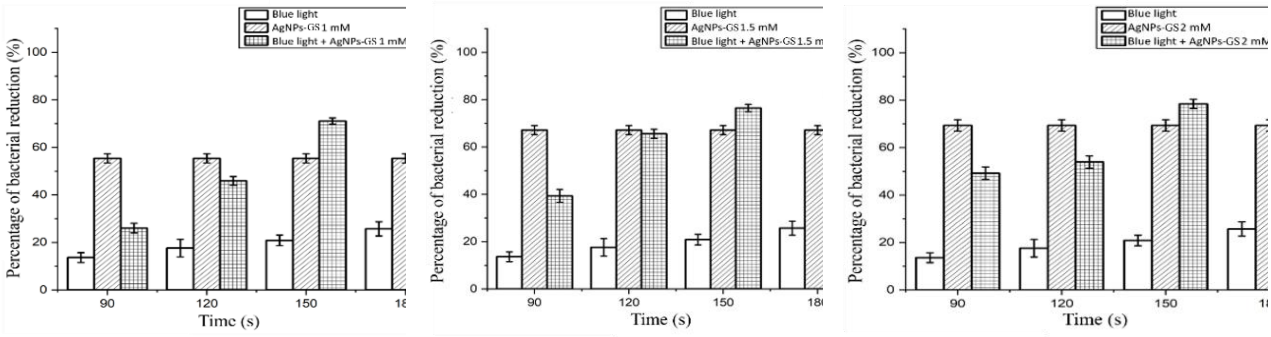

(a) (b) (c)

Figure 10 Comparison of the percentage reduction of *S. aureus* bacteria with AgNPs-Gs (a) 1 mM, (b) 1.5 mM and (c) 2 mM.

Conclusions

Based on the research results, it was found that treatment with grape seed extract silver nanoparticles at a concentration of 2 mM resulted in a 55.78 % reduction in *E. coli* bacterial biofilm and a 68.21 % reduction in *S. aureus* bacterial biofilm. Treatment using 405 nm blue diode laser irradiation led to an 83.26 % reduction with an exposure time of 180 s and a dose of 3.43 J/cm^2. Combining 2 mM grape seed extract silver nanoparticles and blue diode laser irradiation produced the most significant reduction, with a 72.59 % reduction in *E. coli* bacterial biofilm and an 86.74 % reduction in *S. aureus* bacterial biofilm. Therefore, combining blue diode laser and AgNPs-Gs nano photosensitizer yielded the best biofilm reduction effect.

Acknowledgements

This research was funded by a doctoral dissertation grant from the Directorate of Research,

Technology and Community Service 2024 number 1228/UN3/2024.

References

[1] Z Bhutta and S Syed. Diarrheal diseases. *Encyclopedia of Food and Health* 2015; **22**, 361-372.

[2] PC Okhuysen and HL DuPont. Enteroaggregative *Escherichia coli* (EAEC): A cause of acute and persistent diarrhea of worldwide importance. *The Journal of Infectious Diseases* 2010; **202(4)**, 503-505.

[3] O Scudiero, M Brancaccio, C Mennitti, S Laneri, B Lombardo, MGD Biasi and R Pero. Human defensins: A novel approach in the fight against skin colonizing staphylococcus aureus. *Antibiotics* 2020; **9**, 198.

[4] AJ Browne, MG Chipeta, G Haines-Woodhouse EP Kumaran, BHK Hamadani and S Zaraa. Global antibiotic consumption and usage in humans, 2000 - 18: A spatial modelling study. *The Lancet Planetary Health* 2021; **5(12)**, e893-e904.

[5] M Frieri, K Kumar and A Boutin. Antibiotic resistance. *Journal of Infection and Public Health* 2017; **10(4)**, 369-378.

[6] SW Garini, SD Astuti, I Kusumawati and Y Susilo. Combination of curcumin photosensitizer with laser diode to reduce antibiotic resistant bacterial biofilms. *Malaysian Journal of Medicine and Health Sciences* 2021; **17**, 78-81.

[7] N Høiby, T Bjarnsholt, M Givskov S Molin and O Ciofu. Antibiotic resistance of bacterial biofilms. *International Journal of Antimicrobial Agents* 2010; **35(4)**, 322-332.

[8] S Roy, I Hasan and B Guo. Recent advances in nanoparticle-mediated antibacterial applications. *Coordination Chemistry Reviews* 2023; **482**, 215075.

[9] L Rozykulyyeva, SD Astuti, AH Zaidan, AAS Pradhana and PS Puspita. Antibacterial activities of green synthesized silver nanoparticles from *Punica granatum* peel extract. *AIP Conference Proceedings* 2020; **2314(1)**, 060012.

[10] SD Astuti, IW Widya, D Arifianto and R Apsari. Effectiveness photodynamic inactivation with wide spectrum range of diode laser to Staphylococcus aureus bacteria with endogenous photosensitizer: An in vitro study. Journal of International Dental and Medical Research 2019; 12(2): 481-486.

[11] AK Yaqubi, SD Astuti, AH Zaidan, A Syahrom and DZI Nurdin. Antibacterial effect of red laser-activated silver nanoparticles synthesized with grape seed extract against *Staphylococcus aureus* and *Escherichia coli*. *Lasers in Medical Science* 2024; **39(1)**, 47.

[12] MR Khan, KM Fromm, TF Rizvi, B Giese, F Ahamad, RJ Turner, M Füeg and E Marsili. Metal nanoparticle - microbe interactions: Synthesis and antimicrobial effects. *Particle & Particle Systems Characterization* 2020; **37(5)**, 1900419.

[13] MS Tufail and I Liaqat. Silver nanoparticles and their applications - a comprehensive review. *Pure and Applied Biology* 2022; **11(1)**, 315-330.

[14] A Roy, O Bulut, S Some, AK Mandal and MD Yilmaz. Green synthesis of silver nanoparticles: Biomolecule-nanoparticle organizations targeting antimicrobial activity. *RSC Advances* 2019; **9(5)**, 2673-2702.

[15] A Sangwan, H Kumar, A Yadav, J Rani and R Kumar. Evaluation of antibacterial efficacy of iron oxide nanoparticles against *Vibrio vulnificus*: A comparative study with standard antibiotics. *Journal of the Indian Chemical Society* 2024; **101(12)**, 101457.

[16] SD Astuti, DH Kharisma, S Kholimatussa'Diah and AH Zaidan. An *in vitro* antifungal efficacy of silver nanoparticles activated by diode laser to *Candida albicans*. *AIP Conference Proceedings* 2017; **1888**, 020016.

[17] AS Joshi, P Singh and I Mijakovic. Interactions of gold and silver nanoparticles with bacterial biofilms: Molecular interactions behind inhibition and resistance. *International Journal of Molecular Sciences* 2020; **21(10)**, 7658.

[18] D Bamal, A Singh, G Chaudhary, M Kumar, M Singh, N Rani, P Mundlia and AR Sehrawat. Silver nanoparticles biosynthesis, characterization, antimicrobial activities, applications, cytotoxicity and safety issues: An updated review. *Nanomaterials* 2021; **11(8)**, 2086.

[19] A Bouafia, SE Laouini, AS Ahmed, AV Soldatov, H Algarni, KF Chong and GAM Ali. The recent progress on silver nanoparticles: Synthesis and

electronic applications. *Nanomaterials* 2021; **11(9)**, 2318.

[20] A Sharma, H Kumar, C Saini, D Yadav, K Yadav, A Kumar and G Rani. Revolutionizing material science: Enhanced functionalities through reduced graphene oxide/Al_2O_3/CuO/TiO_2 nanocomposites. *Journal of Molecular Structure* 2025; **1323**, 140763.

[21] S Ying, Z Guan, PC Ofoegbu, P Clubb, C Rico, F He and J Hong. Green synthesis of nanoparticles: Current developments and limitations. *Environmental Technology & Innovation* 2022; **26**, 102336.

[22] I Imelda, SD Astuty, PL Gareso, Z Dwyana, NF Arifin and SD Astuti. Green synthesis of silver nanoparticles using *Moringa oleifera*: Implementation to photoantimicrobial of *Candida albicans* with LED light. *Trends in Sciences* 2024; **21(9)**, 8032-8032.

[23] AK Yaqubi, SD Astuti, AH Zaidan and DZI Nurdin. Blue laser-activated silver nanoparticles from grape seed extract for photodynamic antimicrobial therapy against *Escherichia coli* and *Staphylococcus aureus*. *Journal of Lasers in Medical Sciences* 2023; **14**, e69.

[24] S Al-Zahrani, S Astudillo-Calderón, B Pintos, E Pérez-Urria, JA Manzanera, L Martín and A Gomez-Garay. Role of synthetic plant extracts on the production of silver-derived nanoparticles. *Plants* 2021; **10(8)**, 1671.

[25] HR El-Seedi, RM El-Shabasy, SAM Khalifa, A Saeed, A Shah, R Shah, FJ Iftikhar, MM Abdel-Daim, A Omri, NH Hajrahand, JSM Sabir, X Zou, MF Halabi, W Sarhan and W Guo. Metal nanoparticles fabricated by green chemistry using natural extracts: Biosynthesis, mechanisms, and applications. *RSC Advances* 2019; **9**, 24539-24559.

[26] F Al-Otibi, SK Alkhudhair, RI Alharbi, AA Al-Askar, RM Aljowaie and S Al-Shehri. The antimicrobial activities of silver nanoparticles from aqueous extract of grape seeds against pathogenic bacteria and fungi. *Molecules* 2021; **26(19)**, 6081.

[27] A Michalak. Phenolic compounds and their antioxidant activity in plants growing under heavy metal stress. *Polish Journal of Environmental Studies* 2006; **15(4)**, 523-530.

[28] R Majumdar, BG Bag and N Maity. *Acacia nilotica* (Babool) leaf extract mediated size-controlled rapid synthesis of gold nanoparticles and study of its catalytic activity. *International Nano Letters* 2013; **3**, 53.

[29] R Sharma, H Kumar, D Yadav, C Saini, R Kumari, G Kumar, AB Kajjam, V Pandit, M Ayoub, Saloni, Y Deswal and AK Sharma. Synergistic advancements in nanocomposite design: Harnessing the potential of mixed metal oxide/reduced graphene oxide nanocomposites for multifunctional applications. *Journal of Energy Storage* 2024; **93**, 112317.

[30] SD Astuti, A Zaidan, EM Setiawati and Suhariningsih. Chlorophyll mediated photodynamic inactivation of blue laser on *Streptococcus mutans. AIP Conference Proceedings* 2016; **1718(1)**, 120001.

[31] SD Astuti, IB Utomo, EM Setiawatie, M Khasanah, H Purnobasuki, D Arifianto and KA Alamsyah. Combination effect of laser diode for photodynamic therapy with doxycycline on a wistar rat model of periodontitis. *BMC Oral Health* 2021; **21**, 80.

[32] I Yoon, JZ Li and YK Shim. Advance in photosensitizers and light delivery for photodynamic therapy. *Clinical Endoscopy* 2013; **46(1)**, 7-23.

[33] ET Carrera, HB Dias, SCT Corbi, RAC Marcantonio, ACA Bernardi, VS Bagnato, MR Hamblin and ANS Rastelli. The application of antimicrobial photodynamic therapy (aPDT) in dentistry a critical review. *Physiology & Behavior* 2017; **176**, 100-106.

[34] PAD Permatasari, SD Astuti, AK Yaqubi, EAW Paisei and N Anuar. Effectiveness of Katuk leaf chlorophyll (*Sauropus androgynus* (L) merr) with blue and red laser activation to reduce Aggregatibacter actinomycetemcomitans and *Enterococcus faecalis* biofilm. *Biomedical Photonics* 2023; **12(1)**, 14-21.

[35] SD Astuti, A Sulistyo, EM Setiawatie, M Khasanah, H Purnobasuki, D Arifianto, Y Susilo, KA Alamsyah, Suhariningsih and A Syahrom. An *in-vivo* study of photobiomodulation using 403 nm

and 649 nm diode lasers for molar tooth extraction wound healing in wistar rats. *Odontology* 2022; **110**, 240-253.

[36] A Yadav, H Kumar, P Kumar, G Rani and S Maken. *Syzygium cumini* leaf extract mediated green synthesis of ZnO nanoparticles: A sustained release for anticancer, antimicrobial, antioxidant, and anti-corrosive applications. *Journal of Molecular Structure* 2025; **1325**, 141017.

[37] T Siddiqui, MK Zia, M Muaz, H Ahsan and FH Khan. Synthesis and characterization of silver nanoparticles (AgNPs) using chemico-physical methods. *Indonesian Journal of Chemical Analysis* 2023; **6(2)**, 124-132.

[38] H Yang, YY Ren, T Wang and C Wang. Preparation and antibacterial activities of $Ag/Ag^{+}/Ag^{3+}$ nanoparticle composites made by pomegranate (*Punica granatum*) rind extract. *Results in Physics* 2016; **6**, 299-304.

[39] R Sharma, H Kumar, R Kumari, G Kumar, B Swami, A Kumar and R Kumar. Next-generation nanocomposites: Optimizing Al_2O_3-CuO-ZnO and reduced graphene oxide for enhanced performance. *Next Nanotechnology* 2025; **7**, 100119.

[40] S Sajjad, SAK Leghari, NUA Ryma and SA Farooqi. *Green synthesis of metal-based nanoparticles and their applications. In*: S Kanchi and S Ahmed (Eds.). Green metal nanoparticles. Scrivener Publishing, Massachusetts, 2018, p. 23-77.

[41] K Loza, J Diendorf, C Sengstock, L Ruiz-Gonzalez, JM Gonzalez-Calbet, M Vallet-Regi, M Köller and M Epple. The dissolution and biological effects of silver nanoparticles in biological media. *Journal of Materials Chemistry B* 2014; **2**, 1634-1643.

[42] KJ Sreeram, M Nidhin and BU Nair. Microwave assisted template synthesis of silver nanoparticles. *Bulletin of Materials Science* 2008; **31**, 937-942.

[43] JY Song and BS Kim. Rapid biological synthesis of silver nanoparticles using plant leaf extracts. *Bioprocess and Biosystems Engineering* 2009; **32**, 79-84.

[44] MA Radzig, VA Nadtochenko, OA Koksharova, J Kiwi, VA Lipasova and IA Khmel. Antibacterial effects of silver nanoparticles on gram-negative bacteria: Influence on the growth and biofilms formation, mechanisms of action. *Colloids and Surfaces B: Biointerfaces* 2013; **102**, 300-306.

[45] TD Raftery, H Lindler and TL McNealy. Altered host cell - bacteria interaction due to nanoparticle interaction with a bacterial biofilm. *Microbial Ecology* 2013; **65**, 496-503.

[46] A Dhayal, H Kumar, S Prakash, A Kumar, M Brahma and M Maruthi. Development of starch/whey protein isolate biofilm incorporated with silver oxide nanoparticles: A multifunctional antioxidant, antibacterial, photocatalytic, and anticancer agent. *Inorganic Chemistry Communications* 2025; **171**, 113661.

[47] S Kwiatkowski, B Knap, D Przystupski, J Saczko, E Kędzierska and K Knap-Czop. Photodynamic therapy-mechanisms, photosensitizers and combinations. *Biomedicine & Pharmacotherapy* 2018; **106**, 1098-1107.

[48] AB Ormond and HS Freeman. Dye sensitizers for photodynamic therapy. *Materials* 2013; **6**, 817-840.

[49] IO Bacellar and MS Baptista. Mechanisms of photosensitized lipid oxidation and membrane permeabilization. *ACS Omega* 2019; **4(6)**, 21636-21646.

[50] R Itri, HC Junqueira, O Mertins and MS Baptista. Membrane changes under oxidative stress: The impact of oxidized lipids. *Biophysical Reviews* 2014; **6**, 47-61.

[51] MQ Mesquita, CJ Dias, MG Neves, A Almeida and MAF Faustino. Revisiting current photoactive materials for antimicrobial photodynamic therapy. *Molecules: A Journal of Synthetic Chemistry and Natural Product Chemistry* 2018; **23(10)**, 2424.

[52] A Yadav and H Kumar. Self-assembled quantum dots decorated polypyrrole based multifunctional nanocomposite. *Colloids and Surfaces A: Physicochemical and Engineering Aspects* 2023; **666**, 131241.